Nonlinearity-Induced Optical Torque

Ivan Toftul, Gleb Fedorovich, Denis Kislov, Kristina Frizyuk, Kirill Koshelev, Yuri Kivshar, and Mihail Petrov

Phys. Rev. Lett. **130**, 243802 — Published 15 June 2023

DOI: 10.1103/PhysRevLett.130.243802

Nonlinearity-induced optical torque

Ivan Toftul,[1,2] Gleb Fedorovich,[2,3] Denis Kislov,[2,4,5] Kristina Frizyuk,[2] Kirill Koshelev,[1] Yuri Kivshar,[1,*] and Mihail Petrov[2,†]

[1] *Nonlinear Physics Center, Research School of Physics, Australia National University, Canberra ACT 2601, Australia*
[2] *School of Physics and Engineering, ITMO University, St. Petersburg 197101, Russia*
[3] *Department of Physics, ETH Zurich, Zurich 8093, Switzerland*
[4] *Riga Technical University, Institute of Telecommunications, Riga 1048, Latvia*
[5] *Center for Photonics and 2D Materials, Moscow Institute of Physics and Technology, Dolgoprudny 141700, Russia*

(Dated: May 23, 2023)

Optically-induced mechanical torque driving rotation of small objects requires the presence of absorption or breaking cylindrical symmetry of a scatterer. A spherical non-absorbing particle cannot rotate due to the conservation of the angular momentum of light upon scattering. Here, we suggest a novel physical mechanism for the angular momentum transfer to non-absorbing particles via nonlinear light scattering. The breaking of symmetry occurs at the microscopic level manifested in *nonlinear negative optical torque* due to the excitation of resonant states at the harmonic frequency with higher projection of angular momentum. The proposed physical mechanism can be verified with resonant dielectric nanostructures, and we suggest some specific realizations.

Introduction. Rotation and spinning of micro- and nanoscale particles is one of the central goals of optical manipulation since the discovery of optical tweezers [1–8], employed for controlling biological objects [9–11], atoms [12, 13], and nanoscale particles [14–19]. A transfer of the angular momentum from light to matter results in a mechanical torque acting on a scatterer [20–23], that is proportional to a difference between the angular momenta absorbed and re-scattered by the object. Nonzero mechanical torque can appear due to a lack of the rotational symmetry [24–27] or the presence of absorption [28, 29]. Direction and sign of the induced mechanical torque is defined by imbalance conditions, and it can be opposite to the projection of the incident angular moment of light thus generating *negative optical torque* (NOT) [30, 31]. The appearance of linear NOT has recently been studied both theoretically [30, 32, 33] and experimentally [34–37].

Rapid development of all-dielectric nanophotonics [38–41] brings novel opportunities for optical manipulation. In contrast to nanoplasmonics, dielectric materials have lower Ohmic losses [42], which are required for realizing optical rotation of cylindrically symmetric structures [28, 29]. However, dielectric structures offer unique opportunities for observing nonlinear optical processes such as second harmonic generation (SHG) or third-harmonic generation (THG) due to large values of bulk nonlinear susceptibilities. It is also possible to observe experimentally SHG in trapped particles [43, 44]. Recently, the dramatic enhancement of the SHG efficiency for resonant all-dielectric nanostructures was reported [45–50]. Here, we suggest utilizing SHG for a transfer of angular momenta of light to scatterers via nonlinear optical process. The generated *second harmonic (SH) field also may carry the angular momenta* and, thus, provides a contribution to the mechanical torque. We predict that the angular momentum imbalance between the fields at the fundamental and SH frequencies can lead to an optical torque even for non-absorbing particles with cylindrical symmetry (Fig. 1), and its sign can change from positive to *negative* with respect to the incident field angular momentum.

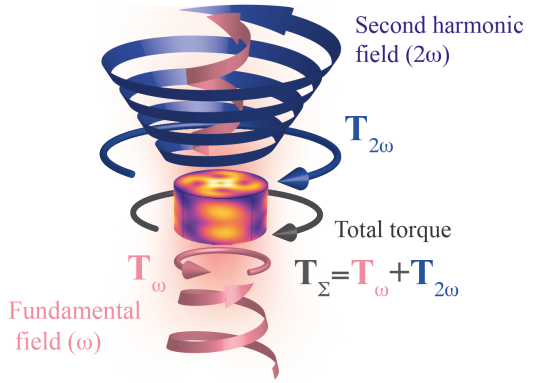

FIG. 1. General concept. Circularly polarized light at the frequency ω is launched onto a cylindrical dielectric particle and generates second-harmonic fields at the frequency 2ω that might have different angular momentum due to a crystalline lattice structure, producing a nonlinearity-induced optical torque enhanced by the Mie resonances.

Nonlinearity-induced optical torque. The circularly polarized plane wave at the frequency ω incident on a dielectric particle possessing the azimuthal symmetry along the axis (see Fig. 1) carries the momentum of light of $m_{\text{inc}}\hbar$ per photon. Due to the symmetry of the problem the optical torque $\mathbf{T}^{(\omega)}$ acting on the particle at the fundamental frequency is exactly proportional to the absorption cross section [28, 29] and, in terms of canonical spin angular momenta density, one can write $\mathbf{T}^{(\omega)} = c/n_0 \cdot \sigma_{\text{abs}}\mathbf{S}^{(\omega)}$. Here $\mathbf{S}^{(\omega)} = m_{\text{inc}}/(2\omega) \cdot \varepsilon\varepsilon_0[E_0^{(\omega)}]^2\mathbf{e}_z$ is

the canonical spin angular momenta density [51] with azimuthal number $m_{\rm inc} = \pm 1$ for right(left) circular polarization (RCP, LCP) and $n_0 = \sqrt{\varepsilon\mu}$ is the refractive index of the host media; $\sigma_{\rm abs}$ is the total absorption cross section. For a nonlinear process in dielectric particles, the energy loss at the fundamental harmonic (FH) frequency occurs due to the harmonic generation, so $\sigma_{\rm abs} \to \sigma_{\rm SHG}$. With the consideration of SHG being a dominant nonlinear process [52], one should also account for the angular momenta carried out by the SH field (Fig. 1). Hence, there are two components of the optical nonlinear torque

$$\mathbf{T} = \mathbf{T}^{(\omega)} + \mathbf{T}^{(2\omega)}, \tag{1}$$

where $\mathbf{T}^{(\omega)}$ and $\mathbf{T}^{(2\omega)}$ are the torques generated by the field at the FH and SH. The interference terms with nonzero frequencies are averaged to zero [53, Sec. I]

For the particles possessing a rotational symmetry with negligible Ohmic losses, torque at the FH is defined by the amount of energy spent on the SHG. By decomposing the SH field into the series of vector spherical harmonics (VSH) it is possible to express the SH generation cross section $\sigma_{\rm SHG}$ in terms of the radial electromagnetic energy density in magnetic and electric multipoles in the far field $W^{\rm E}_{mj}$ and $W^{\rm M}_{mj}$ [45, 53]. With that, the torque at the FH is

$$T_z^{(\omega)} = m_{\rm inc} T_0 \frac{\sigma_{\rm SHG}}{\sigma_{\rm geom}} = \frac{m_{\rm inc} T_0}{\sigma_{\rm geom}[k(2\omega)]^2} \sum_{jm} \left(W^{\rm E}_{mj} + W^{\rm M}_{mj}\right), \tag{2}$$

where $k(2\omega) = n_0 2\omega/c$, $\sigma_{\rm geom}$ is the geometric cross section, m and j are the projection and the total angular momentum numbers correspondingly, and $T_0 = 0.5\varepsilon\varepsilon_0[E_0^{(\omega)}]^2\sigma_{\rm geom}/k(\omega)$, is the maximal torque which can be transferred to a plate of area $\sigma_{\rm geom}$ once all momentum of the incident field is absorbed. Coefficients $W^{\rm E}_{mj}$ and $W^{\rm M}_{mj}$ depend on the overlap integral between the nonlinear polarization $\mathbf{P}^{(2\omega)} = \varepsilon_0\hat{\chi}^{(2)}\mathbf{E}^{(\omega)}\mathbf{E}^{(\omega)}$ and field of the SH mode in the volume of the particle [53, Sec. II]. Thus, $W^{\rm E}_{mj}$ and $W^{\rm M}_{mj}$ contain all the information about nonlinear response. Here, we use the classical description of the SHG process, which is sufficient in the most nanophotonic scenarios; purely quantum optical effects such as entangled photons generation can be considered by using different approach [54, 55].

The torque at the SH frequency can be derived by the calculating the change of the total angular momenta flux tensor $\hat{\mathcal{M}}^{(2\omega)}$ at the SH as $\mathbf{T}^{(2\omega)} = \oint_\Sigma \hat{\mathcal{M}}^{(2\omega)} \cdot \mathbf{n} dS$ [20, 21, 23, 56–58]. Surface integration is performed over arbitrary closed surface Σ which contains the scatterer, and $\mathbf{n}$ is the outer normal to that surface. This integral can be taken once the fields are decomposed into the VSH series [59–62] and the total torque can be written in a compact and elegant way which underpins the physics behind nonlinearity-induced optical torque [53, Sec. I]:

$$\begin{aligned} T_z &= T_z^{(\omega)} + T_z^{(2\omega)} \\ &= \frac{1}{2} T_0 \frac{1}{\sigma_{\rm geom}[k(2\omega)]^2} \sum_{jm} (2m_{\rm inc} - m) \left[W^{\rm E}_{mj} + W^{\rm M}_{mj}\right]. \end{aligned} \tag{3}$$

Eq. (3) is the central result of this work. Generation of a SH photon in the particular VSH state results in *(i)* adding torque corresponding to the spins of two photons absorbed at the FH and *(ii)* adding recoil torque from SH photons emitted with the total angular momentum projection m. This nonlinear optomechanical effect has not been discussed in the literature and is proposed for the first time, to the best of our knowledge.

Selection rules. For the in-depth analysis of Eq. (3) we use the symmetry analysis and multipolar decomposition [45, 63–66]. The imbalance between the angular momentum projections in Eq. (3) immediately shows that there can appear a nonzero torque induced by nonlinear optical generation process. Its sign with respect to $m_{\rm inc}$ strongly depends on the exact multipolar content of the SH field. Most of these components are zero due to the strict selection rules on m during SHG [45, 65, 67–70] imposed by the symmetry of the particle and the crystalline lattice, which can be explicitly seen from the overlapping integral in $W^{\rm E,H}_{mj}$ [53, Sec. II]. In order to illustrate the

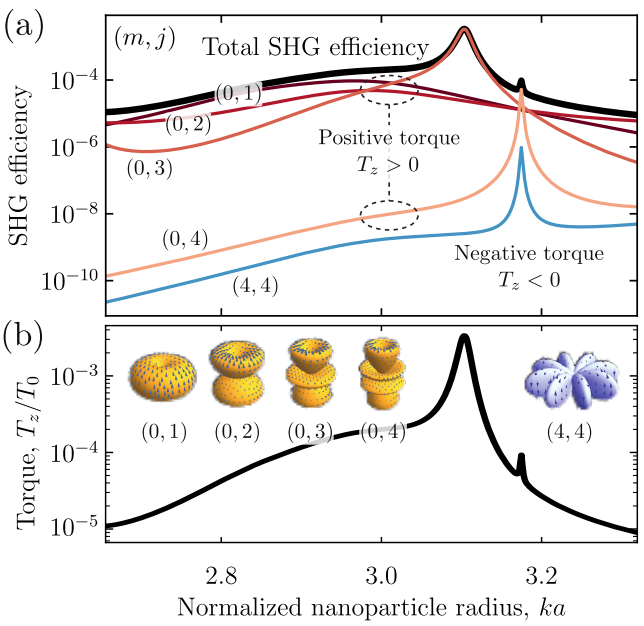

FIG. 2. (a) SHG efficiency ($\sigma_{\rm SHG}/\sigma_{\rm geom}$) in a spherical GaAs nanoparticle with refractive indices $n_{\rm p}^{(\omega)} = 3.28$, $n_{\rm p}^{(2\omega)} = 3.56$ as a function of its radius. The colored lines show the contribution of different multipolar channels labeled as (m, j). The pump wavelength is 1550 nm. The multipoles with $m = 0$ and $m = 4$ provide contribution to positive and negative optical torques, respectively. (b) Total optical torque acting on the spherical nanoparticle, which is positive due to the predominant $m = 0$ contribution.

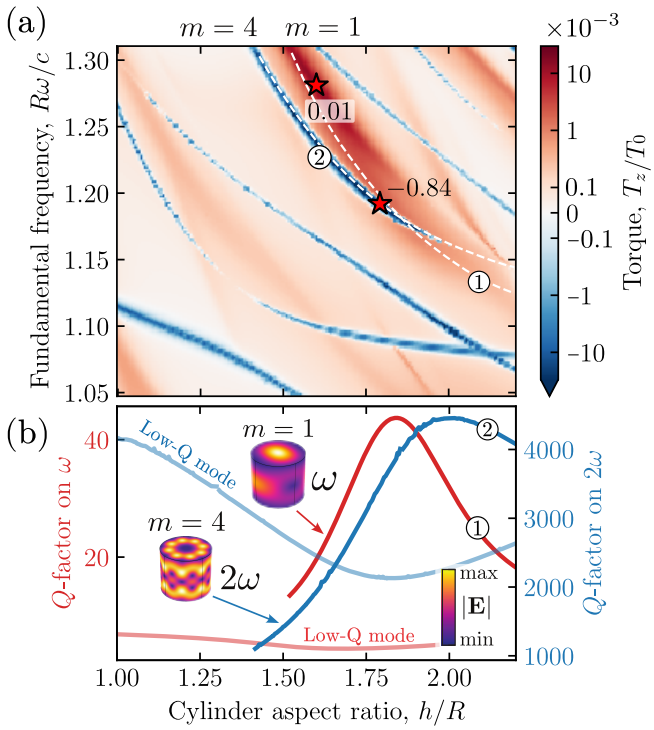

FIG. 3. (a) Total spinning torque at a cylinder with radius $R = 250$ nm made of GaAs with refractive index $n_\mathrm{p} = 3.5$ as a function of dimensionless fundamental frequency $R\omega/c$ and aspect ratio h/R, where h is the cylinder height. Two red stars shows maximal positive and maximal negative values of the torque. Notably, the maximal negative torque coincides with the condition of double resonant mode excitation at the FH and the SH. (b) The Q-factors of these eigenmodes are shown, which have $m = 4$ at the SH and $m = 1$ at the FH. Light blue and light red lines show the Q-factors of the leaky modes near high-Q modes. Electric field amplitude is $E_0^{(\omega)} = 8.68 \cdot 10^7$ V/m.

mechanism of NOT appearance, we consider individual crystalline structures made of GaAs, a common optical material possessing strong second-order nonlinear optical response. Its zinc-blende lattice structure with $\mathrm{T_d}$ symmetry provides a single independent component of the nonlinear tensor $\chi^{(2)}_{xyz}$ [71–74] once the lattice is oriented such that $[001] \parallel \hat{\mathbf{e}}_z, [100] \parallel \hat{\mathbf{e}}_x$.

The symmetry of GaAs lattice along with the axial symmetry of the nanoparticle dictates that only $m = 0, \pm 4$ for incident RCP (LCP) wave are allowed in the SH field, i.e. $2m_\mathrm{inc}$ coming from the incident field and ± 2 from the $\hat{\chi}^{(2)}_\mathrm{GaAs}$ tensor (see Supplemental Materials (SM) [53, Sec. III], and Refs. [45, 75]). From Eq. (3) one can see that for the RCP incident field, which has azimutal number $m_\mathrm{inc} = 1$, harmonics with $m = 0$ provide a positive contribution to the total torque since $2m_\mathrm{inc} - m = 2$ ($T_z^{(\omega)} > 0$, $T_z^{(2\omega)} = 0$), while with $m = 4$ provide a negative contribution since $2m_\mathrm{inc} - m = -2$ ($T_z^{(2\omega)} = -2T_z^{(\omega)}$) and the recoil torque at the SH overcomes the torque at the FH. We emphasize that negative contribution of the mode with $m = 4$ is the consequence of the lattice symmetry, for other materials negative contribution would vary.

We next apply these selection rules to the SHG in a spherical GaAs particle. The particle radius was chosen in the range from 200 nm to 250 nm at the excitation wavelength of 1550 nm. For chosen parameters the excitation is resonant with magnetic dipole mode at the fundamental frequency. The SH field has dominant $j = 1 \ldots 4$ multipolar terms shown in Fig. 2 (b) inset, and their contribution in the overall SHG power is shown in Fig. 2 (a), where SHG efficiency $\sigma_\mathrm{SHG}/\sigma_\mathrm{geom}$ is plotted. The magnetic and electric multipole counterparts are not specified in the plot. As discussed above only $m = 0$ and $m = 4$ components are present in the SH field. One can see that the major contribution to the SHG signal is governed by the harmonics with $m = 0$, while the hexadecapolar harmonic $j = 4, m = 4$ providing a negative torque contribution is very weak. Thus, the SHG in GaAs spherical particles results in *positive* optical torque (see Fig. 2 (b)) reproducing the SH efficiency spectra according to Eq. (3). The same will correspond to particles small compared to the wavelength, where direct estimation of the SHG efficiency can be obtained [53, Sec. VII].

Negative optical torque enabled by high-Q modes. The multipole content of the SH field can be modified and controlled by designing the resonator shape [76–78]. In the view of this work, we aim at enhancing the contribution of $m = 4$ modes in the SH field, which can enable appearance of *negative* optical torque. That can be achieved by lifting degeneracy between modes with different m, utilizing Mie modes with the high total angular momentum j and quasi-bound states in the continuum (qBIC) with high-Q factors and ability to enhance light-matter interaction in the nanoscale structures [79–82]. The qBIC states can be easily observed in cylindrical particles by variation of height to radius ratio preserving the axial symmetry of the system. The Friedrich-Wintgen mechanism [83] allows interaction of different modes with the same m via the radiation continuum resulting in the formation of high-Q qBIC modes along with low-Q modes. Fig. 3 (b) shows the Q-factor of the resonant modes tuned at the FH with $m = 1$ and at SH with $m = 4$, which provides a double resonance condition. The dominating contribution of qBIC modes in the SH spectrum immediately leads to the appearance of negative optical torque (see Fig. 3 (a)) close to $m = 4$ modes excitation as soon as the recoil contribution of SHG with $m = 4$ prevails over the torque due to generation of mode with $m = 0$. Moreover, the resonant character of the effect provides switching of the optical torque from positive to negative in a very narrow range of parameters.

Excitation of high-Q resonant states leads to the drastic increase of the second harmonic efficiency and optical torque in accordance to Eq. (2). The estimation based

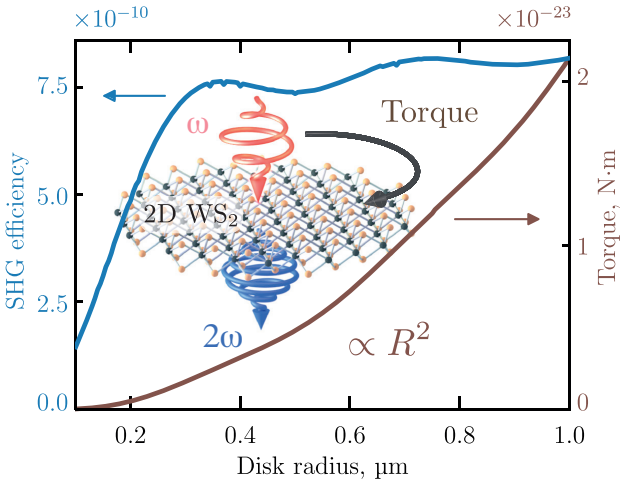

FIG. 4. SHG efficiency $\sigma_{\rm SHG}/\sigma_{\rm geom}$ (blue as a function of the raduis of WS_2 round flake (see inset) and induced nonlinear torque (brown). Amplitude of the incident field is $E_0^{(\omega)} = 8.68 \cdot 10^7$ V/m, and wavelength is 1550 nm.

on the coupled mode theory [81] gives (SM [53, Sec. IV]):

$$\frac{\sigma_{\rm SHG}}{\sigma_{\rm geom}} \simeq 10^{-8} Q_1^2 Q_2 \frac{I_0^{(\omega)}}{1[\rm GW/cm^2]}, \qquad (4)$$

where $I_0^{(\omega)} \approx 1.3$ GW/cm^2 is the intensity of the pump field, the $Q_{1,2}$ are the qBICs Q-factors at the FH and SH, correspondingly (see Fig. 3). In the steady-state regime, the optical torque leads to the rotation of the object at a constant frequency limited by the viscous friction. For a dielectric cylinder in water estimations give us $\Omega_{\rm cyl} \approx 10^5$ rad/s, for the double resonance condition with $Q_1 \approx 50$ and $Q_2 \approx 1000$. We also note that resonant SHG efficiency, and consequently, resonant nonlinear torque are robust to small shape perturbations, for instance, surface roughness or deviations from the cylindrical symmetry [53, Sec. VIII].

Rotation of TMDC flakes. The rotation motion of cylindrical structures is unstable for $h/R \gg 1$, losing its top-like stability and preventing experimental observation of the proposed effect. The critical aspect ratio can be found by setting the equal transverse and longitudinal moments of inertia, which gives $h/R = \sqrt{3}$. (see SM [53, Sec. VI]). In this view, the rotation of atomically thin non-absorptive disks made of two-dimensional (2D) material is deprived of such limitation. The transition metal dichalogenides (TMDC) are known as an efficient platform for flat nonlinear optics [84]. The recent experimental successes in TMDC stable floating on top of liquids [85, 86] inspires us for suggesting the potential geometry of the experiment shown in Fig. 4. The circle structure cut of 2D TMDC flake floating over liquid and illuminated by the laser and resulting in the SHG. The D_{3h} symmetry of the crystalline lattice provides the following nonzero components of a nonlinear tensor $\chi^{(2)}_{xxx} = -\chi^{(2)}_{xyy} = -\chi^{(2)}_{yyx} = -\chi^{(2)}_{yxy} = \chi^{(2)}_{2D}$ [72], which provide that SH modes with $m = \mp 1$ are dominantly generated under right(left) $m_{\rm inc} = \pm 1$ circular excitation [72]. Then the difference between the angular momenta of the generated SH field and the incident field is always negative and the torque is directed along with the incident angular momenta (positive optical torque) and equals to $T_z = \pm 2c/n_0 \cdot \sigma_{\rm SHG}$. In Fig. 4 the dependence of the SHG efficiency on the radius of the TMDC structure is shown. The pump wavelength is 1550 nm with the pump power flux of 2 GW/cm^2 which also lies below the two-photon absorption threshold. The nonlinear tensor coefficient is $\chi^{(2)}_{2D} = 50$ pm/V [87], while the refractive index at the FH and SH frequencies is 2.75 and 3.12, respectively, which corresponds to WS_2 material. From Fig. 4 (b) one can see that the SHG efficiency tends to a constant value with the increase of the structure size corresponding to the efficiency of an infinite sheet. The torque related to the generation of the SH increases quadratically with the structure size. The estimation of the rotation frequency gives $\Omega_{\rm 2D} \approx 0.1$ rad/s [53, Sec. IV].

Discussions. The proposed mechanism of nonlinear optical torque occurs due to the breaking cylindrical symmetry accounting for the crystal lattice symmetry. Indeed, in the SHG process the rule of the momentum projection conservation is satisfied [88] with correction to additional momentum provided by the susceptibility tensor written in the cylindrical coordinates [53, Sec. III]. The proposed mechanism of nonlinearity-induced torque can be observed via other nonlinear processes such as the THG or higher-harmonic generation. For example, for silicon nanostructures (O_h lattice symmetry) the SHG process is suppressed while THG is quite strong. The $\hat{\chi}^{(3)}$ tensor provides the additional momentum $m = \pm 4$ in the third harmonic field in full analogy to the SHG. We also should stress that the THG in isotropic materials will not induce optical torque as the $\hat{\chi}^{(3)}$ tensor has specific form [72] which does not give additional angular momenta projection to the field.

Finally, the generation of nonlinear torque requires strong excitation intensities such that multiphoton absorption can contribute into overall losses [89]. Thus, the proposed nonlinearity-induced mechanism becomes dominant once the two-photon energy is below the band gap $2\hbar\omega < E_g$ (see discussion in SM [53, Sec. V]).

Conclusion. We have presented a general theory of nonlinearity-induced optical torque, originating from the angular momentum transfer from the photonic field to a nanostructure via harmonics generation. We have demonstrated that a nonzero optical torque can appear for the case of a non-absorptive dielectric structures with a rotational symmetry, and the resulting angular frequency can be as high as 100 kHz. Additionally, we have predicted stable rotation of circular TMDC flakes of single-layer WS_2 excited by circularly polarized light.

We believe that our work paves a way towards novel intriguing nonlinear phenomena in optomechanical manipulation.

The authors are indebted to K. Dholakia, R. Quidant, and A. Solntsev for useful comments and references. This work was partially supported by the Program Priority 2030. D.K. acknowledges a support from the Latvian Council of Science (project No. lzp-2022/1-0579). I.T. and Y.K. acknowledge a support from the Australian Research Council (the grant DP210101292) and the International Technology Center Indo-Pacific (ITC IPAC) via Army Research Office (contract No. FA520921P0034). The theoretical analysis of SHG induced torque was supported by the Russian Science Foundation (Grant No. 20-72-10141). The numerical modeling of optomechanical action on high-Q Mie resonators was supported by the Russian Science Foundation (Grant No. 22-42-04420). M.P. acknowledges support from the Foundation for the Advancement of Theoretical Physics and Mathematics "BASIS".

* yuri.kivshar@anu.edu.au
† m.petrov@metalab.ifmo.ru

[1] A. Ashkin, Acceleration and Trapping of Particles by Radiation Pressure, Phys. Rev. Lett. **24**, 156 (1970).
[2] A. Ashkin and J. M. Dziedzic, Optical Levitation by Radiation Pressure, Appl. Phys. Lett. **19**, 283 (1971).
[3] A. Ashkin and J. M. Dziedzic, Stability of optical levitation by radiation pressure, Appl. Phys. Lett. **24**, 586 (1974).
[4] A. Ashkin and J. M. Dziedzic, Optical Levitation of Liquid Drops by Radiation Pressure, Science **187**, 1073 (1975).
[5] A. Ashkin, J. M. Dziedzic, J. E. Bjorkholm, and S. Chu, Observation of a single-beam gradient force optical trap for dielectric particles, Opt. Lett. **11**, 288 (1986).
[6] S. Chu, L. Hollberg, J. E. Bjorkholm, A. Cable, and A. Ashkin, Three-dimensional viscous confinement and cooling of atoms by resonance radiation pressure, Phys. Rev. Lett. **55**, 48 (1985).
[7] J. P. Gordon and A. Ashkin, Motion of atoms in a radiation trap, Phys. Rev. A **21**, 1606 (1980).
[8] A. Ashkin, Trapping of Atoms by Resonance Radiation Pressure, Phys. Rev. Lett. **40**, 729 (1978).
[9] H. Zhang and K.-K. Liu, Optical tweezers for single cells, J. R. Soc. Interface **5**, 671 (2008).
[10] K. Dholakia, B. W. Drinkwater, and M. Ritsch-Marte, Comparing acoustic and optical forces for biomedical research, Nat. Rev. Phys. **2**, 480 (2020).
[11] F. M. Fazal and S. M. Block, Optical tweezers study life under tension, Nat. Photonics **5**, 318 (2011).
[12] A. M. Kaufman and K.-K. Ni, Quantum science with optical tweezer arrays of ultracold atoms and molecules, Nat. Phys. **17**, 1324 (2021).
[13] M. E. Kim, T.-H. Chang, B. M. Fields, C.-A. Chen, and C.-L. Hung, Trapping single atoms on a nanophotonic circuit with configurable tweezer lattices, Nat. Commun. **10**, 1 (2019).
[14] O. M. Maragò, P. H. Jones, P. G. Gucciardi, G. Volpe, and A. C. Ferrari, Optical trapping and manipulation of nanostructures, Nat. Nanotechnol. **8**, 807 (2013).
[15] Y. Shi, Q. Song, I. Toftul, T. Zhu, Y. Yu, W. Zhu, D. P. Tsai, Y. Kivshar, and A. Q. Liu, Optical manipulation with metamaterial structures, Appl. Phys. Rev. **9**, 031303 (2022).
[16] N. Kostina, M. Petrov, A. Ivinskaya, S. Sukhov, A. Bogdanov, I. Toftul, M. Nieto-Vesperinas, P. Ginzburg, and A. Shalin, Optical binding via surface plasmon polariton interference, Phys. Rev. B **99**, 125416 (2019).
[17] G. Tkachenko, G. Tkachenko, I. Toftul, C. Esporlas, A. Maimaiti, A. Maimaiti, A. Maimaiti, F. Le Kien, V. G. Truong, V. G. Truong, S. N. Chormaic, S. N. Chormaic, and S. N. Chormaic, Light-induced rotation of dielectric microparticles around an optical nanofiber, Optica **7**, 59 (2020).
[18] I. D. Toftul, D. F. Kornovan, and M. I. Petrov, Self-Trapped Nanoparticle Binding via Waveguide Mode, ACS Photonics **7**, 114 (2020).
[19] S. Lepeshov, N. Meyer, P. Maurer, O. Romero-Isart, and R. Quidant, Levitated Optomechanics with Meta-Atoms, arXiv 10.48550/arXiv.2211.08235 (2022), 2211.08235.
[20] J. D. Jackson, *Classical Electrodynamics*, Vol. 1 (1998).
[21] L. Novotny and B. Hetch, *Principles of Nano-Optics*, Vol. 1 (2010).
[22] S. M. B. L. Allen, *Optical Angular Momentum* (Taylor & Francis, Andover, England, UK, 2014).
[23] Q. Ye and H. Lin, On deriving the Maxwell stress tensor method for calculating the optical force and torque on an object in harmonic electromagnetic fields, Eur. J. Phys. **38**, 045202 (2017).
[24] E. Brasselet and S. Juodkazis, Optical angular manipulation of liquid crystal droplets in laser tweezers, J. Nonlinear Opt. Phys. Mater. **18**, 167 (2009).
[25] M. E. J. Friese, T. A. Nieminen, N. R. Heckenberg, and H. Rubinsztein-Dunlop, Optical alignment and spinning of laser-trapped microscopic particles, Nature **394**, 348 (1998).
[26] S. H. Simpson, D. C. Benito, and S. Hanna, Polarization-induced torque in optical traps, Phys. Rev. A **76**, 043408 (2007).
[27] J. Trojek, L. Chvátal, and P. Zemánek, Optical alignment and confinement of an ellipsoidal nanorod in optical tweezers: a theoretical study, J. Opt. Soc. Am. A, JOSAA **29**, 1224 (2012).
[28] P. L. Marston and J. H. Crichton, Radiation torque on a sphere caused by a circularly-polarized electromagnetic wave, Phys. Rev. A **30**, 2508 (1984).
[29] A. Canaguier-Durand, A. Cuche, C. Genet, and T. W. Ebbesen, Force and torque on an electric dipole by spinning light fields, Phys. Rev. A **88**, 033831 (2013).
[30] J. Chen, J. Ng, K. Ding, K. H. Fung, Z. Lin, and C. T. Chan, Negative Optical Torque - Scientific Reports, Sci. Rep. **4**, 1 (2014).
[31] Y.-X. Hu, R.-C. Jin, X.-R. Zhang, L.-L. Tang, J.-Q. Li, J. Wang, and Z.-G. Dong, Negative optical torque in spin-dependent 2D chiral nanomotor due to dipolar scattering, Opt. Commun. **482**, 126560 (2021).
[32] F. G. Mitri, Negative optical spin torque wrench of a non-diffracting non-paraxial fractional Bessel vortex beam, J. Quant. Spectrosc. Radiat. Transfer **182**, 172 (2016).

[33] M. Nieto-Vesperinas, Optical torque on small bi-isotropic particles, Opt. Lett. **40**, 3021 (2015).

[34] F. Han, J. A. Parker, Y. Yifat, C. Peterson, S. K. Gray, N. F. Scherer, and Z. Yan, Crossover from positive to negative optical torque in mesoscale optical matter, Nat. Commun. **9**, 1 (2018).

[35] N. Sule, Y. Yifat, S. K. Gray, and N. F. Scherer, Rotation and Negative Torque in Electrodynamically Bound Nanoparticle Dimers, Nano Lett. **17**, 6548 (2017).

[36] K. Diniz, R. S. Dutra, L. B. Pires, N. B. Viana, H. M. Nussenzveig, and P. A. M. Neto, Negative optical torque on a microsphere in optical tweezers, Opt. Express **27**, 5905 (2019).

[37] D. Hakobyan and E. Brasselet, Left-handed optical radiation torque, Nat. Photonics **8**, 610 (2014).

[38] G. P. Zograf, M. I. Petrov, S. V. Makarov, Y. S. Kivshar, and Y. S. Kivshar, All-dielectric thermonanophotonics, Adv. Opt. Photonics **13**, 643 (2021).

[39] D. G. Baranov, D. A. Zuev, S. I. Lepeshov, O. V. Kotov, A. E. Krasnok, A. B. Evlyukhin, and B. N. Chichkov, All-dielectric nanophotonics: the quest for better materials and fabrication techniques, Optica **4**, 814 (2017).

[40] Y. Kivshar, All-dielectric meta-optics and non-linear nanophotonics, Natl. Sci. Rev. **5**, 144 (2018).

[41] A. Krasnok, S. Makarov, M. Petrov, R. Savelev, P. Belov, and Y. Kivshar, Towards all-dielectric metamaterials and nanophotonics, in *Proceedings Volume 9502, Metamaterials X*, Vol. 9502 (SPIE, 2015) p. 950203.

[42] M. Decker and I. Staude, Resonant dielectric nanostructures: a low-loss platform for functional nanophotonics, J. Opt. **18**, 103001 (2016).

[43] L. Malmqvist and H. M. Hertz, Second-harmonic generation in optically trapped nonlinear particles with pulsed lasers, Appl. Opt. **34**, 3392 (1995).

[44] S. Sato and H. Inaba, Second-harmonic and sum-frequency generation from optically trapped KTiOPO4 microscopic particles by use of Nd:YAG and Ti:Al2O3 lasers, Opt. Lett. **19**, 927 (1994).

[45] K. Frizyuk, I. Volkovskaya, D. Smirnova, A. Poddubny, and M. Petrov, Second-harmonic generation in Mie-resonant dielectric nanoparticles made of noncentrosymmetric materials, Phys. Rev. B **99**, 075425 (2019).

[46] K. Koshelev and Y. Kivshar, Dielectric Resonant Metaphotonics, ACS Photonics **8**, 102 (2021).

[47] L. Carletti, S. S. Kruk, A. A. Bogdanov, C. De Angelis, and Y. Kivshar, High-harmonic generation at the nanoscale boosted by bound states in the continuum, Phys. Rev. Res. **1**, 023016 (2019).

[48] L. Carletti, K. Koshelev, C. De Angelis, and Y. Kivshar, Giant Nonlinear Response at the Nanoscale Driven by Bound States in the Continuum, Phys. Rev. Lett. **121**, 033903 (2018).

[49] L. Bonacina, P.-F. Brevet, M. Finazzi, and M. Celebrano, Harmonic generation at the nanoscale, J. Appl. Phys. **127**, 230901 (2020).

[50] S. Wunderlich, B. Schürer, C. Sauerbeck, W. Peukert, and U. Peschel, Molecular Mie model for second harmonic generation and sum frequency generation, Phys. Rev. B **84**, 235403 (2011).

[51] K. Y. Bliokh, A. Y. Bekshaev, and F. Nori, Optical Momentum, Spin, and Angular Momentum in Dispersive Media, Phys. Rev. Lett. **119**, 073901 (2017).

[52] K. M. Ok, E. O. Chi, and P. S. Halasyamani, Bulk characterization methods for non-centrosymmetric materials: second-harmonic generation, piezoelectricity, pyroelectricity, and ferroelectricity, Chem. Soc. Rev. **35**, 710 (2006).

[53] See Supplemental Material at *[URL will be inserted by publisher]* for the optical torque numerical and analytical calculations details, explicit expressions for the coefficients W^{E}_{mj} and W^{H}_{mj}, $\hat{\chi}^{(2)}$ tensor in cylindrical coordinates, estimations of the SHG efficiency and two- and three-photon absorption cross sections, rigid body rotational dynamics simulations, estimations of SHG efficiency in Rayleigh limit, numerical analyses of torque and SH efficiency caused by geometrical anisotropy, and detailed section on complex vector spherical harmonics, which includes Refs [90–120].

[54] A. Nikolaeva, K. Frizyuk, N. Olekhno, A. Solntsev, and M. Petrov, Directional emission of down-converted photons from a dielectric nanoresonator, Phys. Rev. A **103**, 043703 (2021).

[55] A. N. Poddubny, I. V. Iorsh, and A. A. Sukhorukov, Generation of Photon-Plasmon Quantum States in Nonlinear Hyperbolic Metamaterials, Phys. Rev. Lett. **117**, 123901 (2016).

[56] D. J. Griffiths, *Introduction to electrodynamics* (American Association of Physics Teachers, 2005).

[57] J. Mun, M. Kim, Y. Yang, T. Badloe, J. Ni, Y. Chen, C.-W. Qiu, and J. Rho, Electromagnetic chirality: from fundamentals to nontraditional chiroptical phenomena, Light Sci. Appl. **9**, 1 (2020).

[58] A. Y. Bliokh, Konstantin Y.and Bekshaev and F. Nori, Extraordinary momentum and spin in evanescent waves, Nature Communications **5**, 3300 (2014).

[59] Z. Li, Z. Wu, T. Qu, H. Li, L. Bai, and L. Gong, Radiation torque exerted on a uniaxial anisotropic sphere: Effects of various parameters, Opt. Laser Technol. **64**, 269 (2014).

[60] Z.-J. Li, Z.-S. Wu, Q.-C. Shang, L. Bai, and C.-H. Cao, Calculation of radiation force and torque exerted on a uniaxial anisotropic sphere by an incident Gaussian beam with arbitrary propagation and polarization directions, Opt. Express **20**, 16421 (2012).

[61] G. Pesce, P. H. Jones, O. M. Maragò, and G. Volpe, Optical tweezers: theory and practice, Eur. Phys. J. Plus **135**, 1 (2020).

[62] F. Borghese, P. Denti, R. Saija, and M. A. Iatì, Radiation torque on nonspherical particles in the transition matrix formalism, Opt. Express **14**, 9508 (2006).

[63] M. Tsimokha, V. Igoshin, A. Nikitina, I. Toftul, K. Frizyuk, and M. Petrov, Acoustic resonators: Symmetry classification and multipolar content of the eigenmodes, Phys. Rev. B **105**, 165311 (2022).

[64] Z. Sadrieva, K. Frizyuk, M. Petrov, Y. Kivshar, and A. Bogdanov, Multipolar origin of bound states in the continuum, Phys. Rev. B **100**, 115303 (2019).

[65] K. Frizyuk, Second-harmonic generation in dielectric nanoparticles with different symmetries, J. Opt. Soc. Am. B, JOSAB **36**, F32 (2019).

[66] K. Frizyuk, E. Melik-Gaykazyan, J.-H. Choi, M. I. Petrov, H.-G. Park, and Y. Kivshar, Nonlinear Circular Dichroism in Mie-Resonant Nanoparticle Dimers, Nano Lett. **21**, 4381 (2021).

[67] M. Finazzi, P. Biagioni, M. Celebrano, and L. Duò, Selection rules for second-harmonic generation in nanopar-

ticles, Phys. Rev. B **76**, 125414 (2007).
[68] S. V. Makarov, M. I. Petrov, U. Zywietz, V. Milichko, D. Zuev, N. Lopanitsyna, A. Kuksin, I. Mukhin, G. Zograf, E. Ubyivovk, D. A. Smirnova, S. Starikov, B. N. Chichkov, and Y. S. Kivshar, Efficient Second-Harmonic Generation in Nanocrystalline Silicon Nanoparticles, Nano Lett. **17**, 3047 (2017).
[69] D. Smirnova, A. I. Smirnov, and Y. S. Kivshar, Multipolar second-harmonic generation by Mie-resonant dielectric nanoparticles, Phys. Rev. A **97**, 013807 (2018).
[70] J. I. Dadap, Optical second-harmonic scattering from cylindrical particles, Phys. Rev. B **78**, 205322 (2008).
[71] C. S. Smith, Macroscopic Symmetry and Properties of Crystals, in *Solid State Physics*, Vol. 6 (Academic Press, Cambridge, MA, USA, 1958) pp. 175–249.
[72] R. Boyd, *Nonlinear Optics* (Elsevier Science, 2020).
[73] R. C. Miller, Optical second harmonic generation in piezoelectric crystals, Appl. Phys. Lett. **5**, 17 (1964).
[74] P. A. Franken and J. F. Ward, Optical Harmonics and Nonlinear Phenomena, Rev. Mod. Phys. **35**, 23 (1963).
[75] K. Frizyuk, E. Melik-Gaykazyan, J.-H. Choi, M. I. Petrov, H.-G. Park, and Y. Kivshar, Nonlinear Circular Dichroism in Mie-Resonant Nanoparticle Dimers, Nano Lett. **21**, 4381 (2021).
[76] S. Gladyshev, K. Frizyuk, and A. Bogdanov, Symmetry analysis and multipole classification of eigenmodes in electromagnetic resonators for engineering their optical properties, Physical Review B **102**, 75103 (2020).
[77] Z. Sadrieva, K. Frizyuk, M. Petrov, Y. Kivshar, and A. Bogdanov, Multipolar origin of bound states in the continuum, Physical Review B **100**, 1 (2019), arXiv:1903.00309.
[78] T. Liu, R. Xu, P. Yu, Z. Wang, and J. Takahara, Multipole and multimode engineering in Mie resonance-based metastructures, Nanophotonics **0**, 1 (2020).
[79] K. Koshelev, Z. Sadrieva, A. Shcherbakov, Y. Kivshar, and A. Bogdanov, Bound states in the continuum in photonic structures, Uspekhi Fizicheskikh Nauk 10.3367/UFNe.2021.12.039120 (2022), 2207.01441.
[80] M. V. Rybin, K. L. Koshelev, Z. F. Sadrieva, K. B. Samusev, A. A. Bogdanov, M. F. Limonov, and Y. S. Kivshar, High-Q Supercavity Modes in Subwavelength Dielectric Resonators, Phys. Rev. Lett. **119**, 243901 (2017).
[81] K. Koshelev, S. Kruk, E. Melik-Gaykazyan, J.-H. Choi, A. Bogdanov, H.-G. Park, and Y. Kivshar, Subwavelength dielectric resonators for nonlinear nanophotonics, Science **367**, 288 (2020).
[82] A. A. Bogdanov, K. L. Koshelev, P. V. Kapitanova, M. V. Rybin, S. A. Gladyshev, Z. F. Sadrieva, K. B. Samusev, Y. S. Kivshar, and M. F. Limonov, Bound states in the continuum and Fano resonances in the strong mode coupling regime, *Advanced Photonics, 1(1)*, Adv. Photonics **1**, 016001 (2019).
[83] Friedrich H. and Wintgen D., Interfering resonances and BIC, Physical Review A **32**, 3231 (1985).
[84] S. J. McDonnell and R. M. Wallace, Atomically-thin layered films for device applications based upon 2D TMDC materials, Thin Solid Films **616**, 482 (2016).
[85] X.-k. Zhao, R.-w. Chen, K. Xu, S.-y. Zhang, H. Shi, Z.-y. Shao, and N. Wan, Nanoscale water film at a super-wetting interface supports 2D material transfer, 2D Mater. **8**, 015021 (2020).
[86] G. Jin, C.-S. Lee, X. Liao, J. Kim, Z. Wang, O. F. N. Okello, B. Park, J. Park, C. Han, H. Heo, J. Kim, S. H. Oh, S.-Y. Choi, H. Park, and M.-H. Jo, Atomically thin three-dimensional membranes of van der Waals semiconductors by wafer-scale growth, Sci. Adv. **5**, eaaw3180 (2019).
[87] J. W. You, S. R. Bongu, Q. Bao, and N. C. Panoiu, Nonlinear optical properties and applications of 2D materials: theoretical and experimental aspects, Nanophotonics **8**, 63 (2019).
[88] A. Nikitina, A. Nikolaeva, and K. Frizyuk, Nonlinear circular dichroism in achiral dielectric nanoparticles, Phys. Rev. B **107**, L041405 (2023).
[89] W. C. Hurlbut, Y.-S. Lee, K. L. Vodopyanov, P. S. Kuo, and M. M. Fejer, Multiphoton absorption and nonlinear refraction of GaAs in the mid-infrared, Opt. Lett. **32**, 668 (2007).
[90] J. P. Barton, D. R. Alexander, and S. A. Schaub, Internal and near-surface electromagnetic fields for a spherical particle irradiated by a focused laser beam, J. Appl. Phys. **64**, 1632 (1988).
[91] J. P. Barton, D. R. Alexander, and S. A. Schaub, Theoretical determination of net radiation force and torque for a spherical particle illuminated by a focused laser beam, J. Appl. Phys. **66**, 4594 (1989).
[92] P. A. Belov, S. I. Maslovski, K. R. Simovski, and S. A. Tretyakov, A condition imposed on the electromagnetic polarizability of a bianisotropic lossless scatterer, Tech. Phys. Lett. **29**, 718 (2003).
[93] S. Bergfeld and W. Daum, Second-Harmonic Generation in GaAs: Experiment versus Theoretical Predictions of $\chi^{(2)}_{xyz}$, Phys. Rev. Lett. **90**, 036801 (2003).
[94] COMSOL Documentation (2021), [Online; accessed 2. Jun. 2021].
[95] C. F. Bohren and D. R. Huffman, *Absorption and scattering of light by small particles* (John Wiley & Sons, 2008).
[96] C. R. Cantor and P. R. Schimmel, *Biophysical chemistry: Part II: Techniques for the study of biological structure and function* (Macmillan, 1980).
[97] P. C. Chaumet and A. Rahmani, Electromagnetic force and torque on magnetic and negative-index scatterers, Opt. Express **17**, 2224 (2009).
[98] E. A. Coutsias and L. Romero, The Quaternions with an application to Rigid Body Dynamics, UNM Digital Repository (2004).
[99] C. M. De Witt and J. H. D. Jensen, Über den Drehimpuls der Multipolstrahlung, Zeitschrift für Naturforschung A **8**, 267 (1953).
[100] M. B. Doost, W. Langbein, and E. A. Muljarov, Resonant-state expansion applied to three-dimensional open optical systems, Phys. Rev. A **90**, 013834 (2014).
[101] S. H. Koenig, Brownian motion of an ellipsoid. a correction to perrin's results, Biopolymers: Original Research on Biomolecules **14**, 2421 (1975).
[102] K. Koshelev, *Advanced trapping of light in resonant dielectric metastructures for nonlinear optics*, Ph.D. thesis, Australian National University (2022).
[103] G. Kristensson, Spherical vector waves (2014).
[104] L. D. Landau, J. Bell, M. Kearsley, L. Pitaevskii, E. Lifshitz, and J. Sykes, *Electrodynamics of continuous media*, Vol. 8 (elsevier, 2013).

[105] L. D. Landau and E. M. Lifshitz, *Fluid Mechanics: Landau and Lifshitz: Course of Theoretical Physics, Volume 6*, Vol. 6 (Elsevier, 2013).

[106] Z.-J. Li, Z.-S. Wu, and Q.-C. Shang, Calculation of radiation forces exerted on a uniaxial anisotropic sphere by an off-axis incident Gaussian beam, Optics Express **19**, 16044 (2011).

[107] Z.-J. Li, Z.-S. Wu, Q.-C. Shang, L. Bai, and C.-H. Cao, Calculation of radiation force and torque exerted on a uniaxial anisotropic sphere by an incident Gaussian beam with arbitrary propagation and polarization directions, Opt. Express **20**, 16421 (2012).

[108] Z. Li, Z. Wu, T. Qu, H. Li, L. Bai, and L. Gong, Radiation torque exerted on a uniaxial anisotropic sphere: Effects of various parameters, Optics & Laser Technology **64**, 269 (2014).

[109] S. V. Lobanov, W. Langbein, and E. A. Muljarov, Resonant-state expansion applied to three-dimensional open optical systems: Complete set of static modes, Phys. Rev. A **100**, 063811 (2019).

[110] E. A. Muljarov and T. Weiss, Resonant-state expansion for open optical systems: generalization to magnetic, chiral, and bi-anisotropic materials, Opt. Lett. **43**, 1978 (2018).

[111] M. Nieto-Vesperinas, J. J. Sáenz, R. Gómez-Medina, and L. Chantada, Optical forces on small magnetodielectric particles, Opt. Express **18**, 11428 (2010).

[112] M. Nieto-Vesperinas, Optical torque: Electromagnetic spin and orbital-angular-momentum conservation laws and their significance, Phys. Rev. A **92**, 043843 (2015).

[113] F. Perrin, Mouvement brownien d'un ellipsoide - I. Dispersion diélectrique pour des molécules ellipsoidales, J. Phys. Radium **5**, 497 (1934).

[114] H. S. Sehmi, W. Langbein, and E. A. Muljarov, Applying the resonant-state expansion to realistic materials with frequency dispersion, Phys. Rev. B **101**, 045304 (2020).

[115] W. Tang, W. Lyu, J. Lu, F. Liu, J. Wang, W. Yan, and M. Qiu, Micro-scale opto-thermo-mechanical actuation in the dry adhesive regime, Light Sci. Appl. **10**, 1 (2021).

[116] toftul, tensors-in-curvilinear-coordinates (2022), [Online; accessed 18. Jul. 2022].

[117] D. A. Varshalovich, A. N. Moskalev, and V. K. Khersonskii, *Quantum Theory of Angular Momentum* (World Scientific Publishing Company, Singapore, 1988).

[118] T. Weiss and E. A. Muljarov, How to calculate the pole expansion of the optical scattering matrix from the resonant states, Phys. Rev. B **98**, 085433 (2018).

[119] E. W. Weisstein, Condon-Shortley Phase, Wolfram Research, Inc. (2003).

[120] J. Stratton, *Electromagnetic Theory*, IEEE Press Series on Electromagnetic Wave Theory (Wiley, 2007).